Application of the Gillespie algorithm to a granular intruder particle

Application of the Gillespie algorithm to a granular intruder particle

J Talbot[1] **and P Viot**[2]

[1] Department of Chemistry and Biochemistry, Duquesne University, Pittsburgh, PA 15282-1530, USA
[2] Laboratoire de Physique Théorique des Liquides, Université Pierre et Marie Curie, 4, place Jussieu, 75252 Paris Cedex 05, France

Abstract

We show how the Gillespie algorithm, originally developed to describe coupled chemical reactions, can be used to perform numerical simulations of a granular intruder particle colliding with thermalized bath particles. The algorithm generates a sequence of collision 'events' separated by variable time intervals. As input, it requires the position-dependent flux of bath particles at each point on the surface of the intruder particle. We validate the method by applying it to a one-dimensional system for which the exact solution of the homogeneous Boltzmann equation is known and investigate the case where the bath particle velocity distribution has algebraic tails. We also present an application to a granular needle in a bath of point particles where we demonstrate the presence of correlations between the translational and rotational degrees of freedom of the intruder particle. The relationship between the Gillespie algorithm and the commonly used direct simulation Monte Carlo (DSMC) method is also discussed.

PACS numbers: 05.20.−y, 51.10.+y, 44.90.+c

(Some figures in this article are in colour only in the electronic version)

1. Introduction

Kinetic theories of granular systems are usually constructed starting from the Boltzmann equation or one of its variants [1, 2]. Rarely, it is possible to obtain an exact, analytic solution of the Boltzmann equation [3]. More typically, however, approximations are required. It is then highly desirable to assess the quality of the theoretical prediction by comparing it with accurate numerical solutions of the Boltzmann equation. It is the purpose of this paper to show that, besides the celebrated direct simulation Monte Carlo (DSMC) introduced by Bird

[4], there exists an alternative method, originally proposed by Gillespie [5, 6] to study coupled chemical reactions.

One class of system that is amenable to a Boltzmann approach and that has received considerable attention in recent years consists of a single intruder (or tracer) particle in a bath of thermalized particles [7–12], showing in particular the absence of equipartition. This phenomenon has been observed experimentally in two-dimensional [13] and three-dimensional [14] granular gases. The intruder–bath particle collisions are dissipative, while the bath particles have an ideal gas structure and a specified velocity distribution characterized by a fixed temperature. Since Gaussian velocity statistics are quite rare, it is important that numerical and theoretical approaches be able to treat a general distribution.

We begin by outlining the Gillespie algorithm and how it can be used for obtaining a numerical solution of the Boltzmann equation. We then illustrate the application of the algorithm with two examples. The first is a one-dimensional system consisting of an intruder particle in a bath of thermalized point particles. If the bath particles have a Gaussian velocity distribution one recovers the exact Gaussian intruder velocity distribution function [9] with a granular temperature that is smaller than the bath temperature. In addition when we impose a power-law velocity distribution on the bath particles, we find the same form for the intruder particle distribution.

The second system is two dimensional and consists of a needle intruder in a bath of point particles. It is known that equipartition does not hold between different degrees of freedom of the needle [10]. Here we use the Gillespie algorithm to obtain a new physical result, namely the presence of correlations between the translational and rotational degree of freedom of the needle.

2. Algorithm

The model consists of a single intruder particle that undergoes a series of collisions with the surrounding bath particles. Let $P(t)$ denote the probability that no event (collision) has occurred in the interval $(0, t)$. Then

$$P(t + \Delta t) = P(t)(1 - \phi(t)\Delta t + O(\Delta t^2)), \tag{1}$$

where $\phi(t)$ is the event rate in general and the collision rate in this application. Expanding the lhs to first order in Δt and taking the limit $\Delta t \to 0$ leads to

$$\frac{\mathrm{d}\ln P(t)}{\mathrm{d}t} = -\phi(t). \tag{2}$$

Integrating and using the boundary condition that $P(0) = 1$ gives

$$P(t) = \exp\left[-\int_0^t \phi(t')\,\mathrm{d}t'\right]. \tag{3}$$

If $\phi(t)$ is constant between collisions this expression takes the simple form

$$P(t) = \exp(-\phi t). \tag{4}$$

At the end of the waiting time an event (collision) occurs that alters the value of ϕ or the way that ϕ evolves with time. We now consider two specific applications. In the first, the flux of colliding particles is constant between collisions and the simpler form, equation (4) may be used. Our second example, an anisotropic object that rotates between collisions, requires the use of the more general form, equation (3).

3. Applications

3.1. One-dimensional system

Consider first a one-dimensional system consisting of an intruder particle of mass M moving in a bath of thermalized point particles each of mass m. The dynamics of the intruder is described by the Boltzmann equation.

The velocity distribution of the bath particles is denoted by $f(v, a)$, where a is related to the bath temperature, T_B.

The flux of particles that collide with the right hand side of the intruder particle moving with a velocity v_1 is:

$$\phi_+(v_1) = \rho \int_{-\infty}^{v_1} (v_1 - v) f(v, a) \, dv, \tag{5}$$

where ρ is the number density of the bath particles. Similarly the flux on the left-hand side is

$$\phi_-(v_1) = \rho \int_{v_1}^{\infty} (v - v_1) f(v, a) \, dv, \tag{6}$$

and the total collision rate is

$$\phi(v_1) = \phi_+(v_1) + \phi_-(v_1). \tag{7}$$

Let $F(v_1, t)$ denote the time-dependent distribution function of tracer particle velocity. Then this evolves according to

$$\frac{\partial F(v_1, t)}{\partial t} = -\phi(v_1) F(v_1, t) + \int_{-\infty}^{\infty} \psi(v \to v_1) F(v, t) \, dv, \tag{8}$$

which is equivalent to the homogeneous Boltzmann equation [3]. The first term on the rhs is a loss term corresponding to the probability that a tracer particle with velocity v_1 undergoes a collision (necessarily to a different velocity) per unit time. The second, or gain, term contains the function $\psi(v \to v_1)$ that is the rate that tracer particles moving with velocity v are transformed (by collisions with the bath particles) to those moving with velocity v_1. For collisions with the rhs of the intruder particle the explicit expression is

$$\psi_+(v \to v_1) = \rho \left(\frac{1 + M}{1 + \alpha} \right)^2 (v - v_1) f \left(v + \frac{1 + M}{1 + \alpha} (v_1 - v), a \right), \tag{9}$$

with $v_1 < v$. A similar expression applies for collisions on the left-hand side of the intruder particle. We note that a representation of the Boltzmann equation similar to equation (8) was employed by Puglisi *et al* [12].

The Gillespie algorithm provides a numerical solution of equation (8) including the transient case when the derivative is not equal to zero.

If the intruder particle moves with a constant velocity the flux is itself (on average) constant. A waiting time consistent with equation (3) is then generated:

$$\Delta t = -\ln(\xi_1) / \phi(v_1), \tag{10}$$

where $0 < \xi_1 < 1$ is a uniform random number.

Given a collision at time t, the probability that the collision occurs on the right-hand side is given by

$$p(+|t) = \phi_+(v_1) / \phi(v_1). \tag{11}$$

This is sampled by generating a second uniform random number $0 < \xi_2 < 1$. If $\xi_2 < p(+|t)$ the collision is on the right-hand side: otherwise it takes place on the left-hand side.
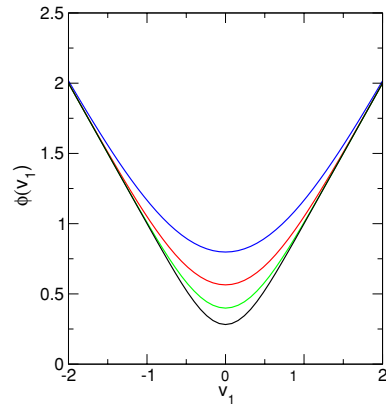
Figure 1. Flux, or collision rate, on both sides of a surface moving in a bath of particles with a Gaussian velocity distribution at a velocity v_1. $a = 0.5, 1, 2, 4$ top to bottom.

Having chosen the side, it is then necessary to sample the velocity of the bath particle that collides with this side. The probability distribution function of the colliding particle's velocity depends on the collision side:

$$g_+(v, v_1) = \begin{cases} (v_1 - v) f(v, a)/\phi_+(v_1) & \text{if } v \leqslant v_1 \\ 0 & \text{otherwise} \end{cases} \tag{12}$$

$$g_-(v, v_1) = \begin{cases} (v - v_1) f(v, a)/\phi_-(v_1) & \text{if } v \geqslant v_1 \\ 0 & \text{otherwise.} \end{cases} \tag{13}$$

The results presented so far apply to any bath velocity distribution—and the behaviour depends strongly on the exact form [12]. For a Gaussian

$$f(v, a) = \sqrt{\frac{a}{\pi}} \exp(-av^2), \qquad -\infty < v < \infty \tag{14}$$

where $a = m/(2k_B T_B)$. The collision fluxes on each side of the tracer particle are

$$\phi_\pm(v_1) = \frac{\rho}{2} \left(\pm v_1 + \frac{1}{\sqrt{\pi a}} \exp\left(-av_1^2\right) + v_1 \, \text{erf}(v_1 \sqrt{a}) \right), \tag{15}$$

and the total collision rate is

$$\phi(v_1) = \rho \left(\frac{1}{\sqrt{\pi a}} \exp\left(-av_1^2\right) + v_1 \, \text{erf}(v_1 \sqrt{a}) \right). \tag{16}$$

This function is shown in figure 1.

The velocity distribution of the colliding particles, equation (12), in the case of a bath particle Gaussian velocity distribution is plotted in figure 2 for several values of the intruder particle velocity. Sampling of this distribution is accomplished with an acceptance–rejection method in which the sampling region is adapted to the velocity of the intruder. A rare, but possible, case is to select a collision on the right hand side when the surface is moving rapidly to the left. The distribution of colliding particles is sharply peaked at v_1 and it is necessary to take the range of v from $v_1 - 2$ to v_1. If the surface is moving to the right, the distribution of colliding particle's velocity is more symmetric and one can sample v in the range $-3 \leqslant v \leqslant 3$.
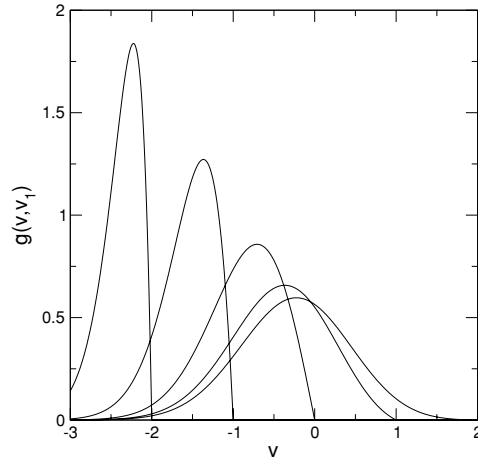
Figure 2. Probability distribution of particles that collide with the right-hand side of a surface moving with a velocity $v_1 = -2, -1, 0, 1, 2$, left to right. The bath particles have a Gaussian velocity distribution.

Finally, when the intruder particle moving with a velocity v_1 collides with a bath particle of velocity v the velocity of the former changes instantaneously to

$$v_1' = v_1 + \frac{1+\alpha}{1+M}(v - v_1), \tag{17}$$

where $0 < \alpha \leqslant 1$ is the coefficient of restitution and we have taken $m = 1$ for convenience.

The complete algorithm describing one iteration can now be summarized using pseudocode:

(1) Generate a waiting time using equation (10).
(2) $t \rightarrow t + \Delta t$

  while $(t_{\text{out}} < t)$

  $\{t_{\text{out}} \leftarrow t_{\text{out}} + \delta t$

  accumulate averages$\}$.

(3) Choose the collision side using equation (11).
(4) The velocity of the colliding bath particle v is sampled from the distribution given by equation (12) or equation (13).
(5) The post-collisional velocity of the intruder particle is determined from equation (17).

Although the time increment between events is variable, averages (mean square velocities and velocity distributions) must be computed at equal time intervals. In step 2, t denotes the total elapsed time, and δt is the constant time interval between the accumulation of quantities to be averaged. A convenient choice for δt is the average collision time.

Martin and Piasecki [9] obtained an analytic solution of the homogeneous stationary Boltzmann equation and showed that the velocity distribution of the intruder particle in the steady state is Gaussian and characterized by a temperature, T, that is different from the bath temperature T_B. Specifically, the two are related by

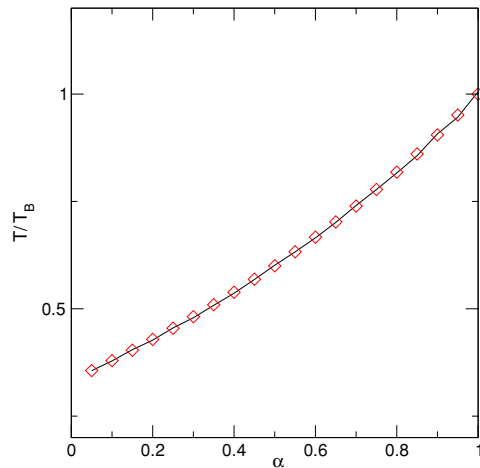$$\frac{T}{T_B} = \frac{1+\alpha}{2 + (1-\alpha)/M}, \tag{18}$$

Figure 3. Ratio of the intruder granular temperature to the bath temperature. Symbols show the simulation results and the solid curve shows the theoretical prediction of Martin and Piasecki, equation (18). Results are for $M = m$ and $n_{col} = 500\,000$.

so that for $\alpha < 1$, $T < T_B$. Figure 3 shows an excellent agreement of the simulation with this exact result.

Since the existence of solutions of the Boltzmann equation with power-law tails has been shown recently [15, 16], it is interesting to investigate this phenomenon in the intruder particle system using the Gillespie algorithm. Therefore, we consider the case where the bath particle velocity distribution function takes the following power-law form:

$$f(a, v) = \frac{\sqrt{2a}}{\pi} \frac{1}{1 + a^2 v^4}. \tag{19}$$

The granular temperature of the bath is well defined since the average of the square velocity is finite, $\langle v^2 \rangle = 1/a$.

Although the Boltzmann equation can no longer be solved in general for an arbitrary bath particle velocity distribution (unlike the just-discussed Gaussian distribution), an exact solution is possible when the mass ratio is equal to the coefficient of restitution, $M/m = \alpha$. For this specific case one can show that the stationary solution of the intruder particle is exactly given by equation (19) [3] with a granular temperature equal to the bath temperature multiplied by the coefficient of restitution.

Figure 4 shows the variation of the granular temperature of the intruder particle with α for $M/m = 1$ and $M/m = 0.5$. When the intruder is light, $M < m$, the granular temperature of the intruder particle is close to the result obtained with the Gaussian bath when $\alpha > M/m$ (see figure 4).

Figure 5 displays the intruder particle velocity distribution function for different values of the coefficient of restitution $0.0 \leqslant \alpha \leqslant 1.0$, when $M = 1/2$. The exact solution is known for $\alpha = 0.5$, i.e. equation (19) with a granular temperature equal to α. The simulation results show that in all cases the velocity distribution functions exhibit a power-law tail (see inset of figure 5) with an exponent independent of α and equal to -4.

3.2. Needle

In this application a needle intruder, confined to a two-dimensional plane, is immersed in a fluid of point particles, each of mass m, at a density ρ. The needle is characterized by its mass
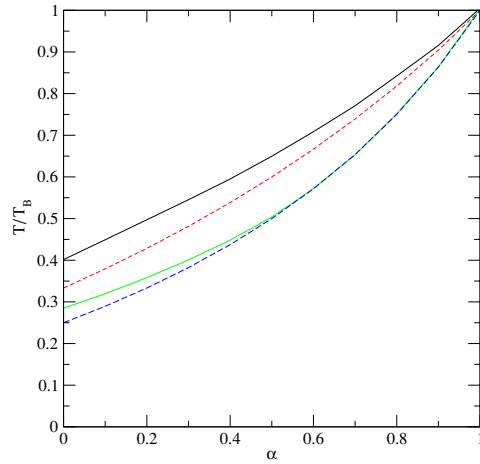
Figure 4. Granular temperatures of the intruder particle normalized by the bath temperature, $T/T_{\rm B}$, versus the coefficient of restitution α when the velocity distribution of the bath is given by equation (19) for $M = 1$ and $M = 0.5$, from top to bottom. Dashed curves correspond to the analytical result [9] when the velocity distribution of the bath is Gaussian.
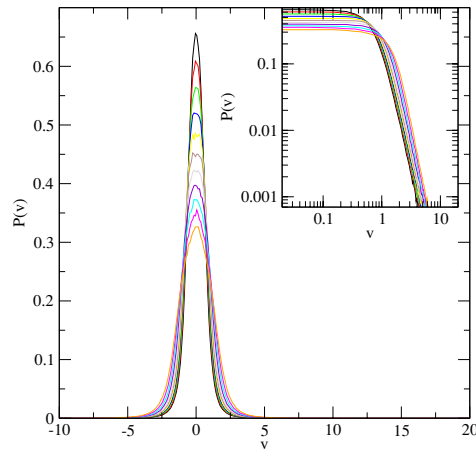

Figure 5. Velocity distribution function of the intruder particle for different values of the coefficient of restitution $\alpha = 0.0, 0.1, 0.2, \ldots, 0.8, 0.9, 1.0$, from top to bottom, when $M = 1/2$ and when the bath distribution is given by equation (19). The insert is a log–log plot showing the algebraic decay of the velocity distribution.

M, length L and moment of inertia I and its state is specified by its angular and centre-of-mass velocities, ω and $\mathbf{v}_1$, respectively (see figure 6). The velocity distribution of the point particles is again given by equation (14).

Two main modifications of the Gillespie algorithm are required in order to simulate this system. First, if $v_1 \neq 0$ the flux is not (on average) constant between collisions. Second, it is necessary to select the point of impact on the needle.

The collision flux on both sides of the needle at a point $-L/2 \leqslant x \leqslant L/2$ is $\phi(\mathbf{v}_1 \cdot \mathbf{n} + \omega x)$. Unlike the case considered above, this flux is time-dependent if $\omega \neq 0$
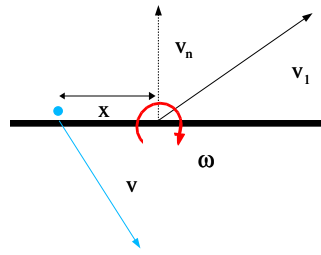
Figure 6. Geometry of the needle-point system.

since the normal vector $\mathbf{n}$ rotates. Specifically

$$v_n = \mathbf{v}_1 \cdot \mathbf{n}(t) = v_{1y} \cos(\omega t + \theta_0) - v_{1x} \sin(\omega t + \theta_0), \tag{20}$$

where θ_0 is the orientation of the needle at $t = 0$. The total flux over the entire length of the needle is

$$\Phi(t) = \int_{-L/2}^{L/2} \phi \left(\mathbf{v}_1 \cdot \mathbf{n}(t) + \omega x \right) \mathrm{d}x. \tag{21}$$

For the sake of simplicity we take $a = 1$ and $L = 1$ and we obtain

$$
\begin{aligned}
\Phi(t) = {} & \rho \left(\frac{v_n^2}{2\omega} + \frac{\omega}{8} + \frac{v_n}{2} + \frac{1}{4\omega} \right) \mathrm{erf} \left(v_n + \frac{\omega}{2} \right) \\
& + \rho \left(\frac{v_n^2}{2\omega} + \frac{\omega}{8} - \frac{v_n}{2} + \frac{1}{4\omega} \right) \mathrm{erf} \left(-v_n + \frac{\omega}{2} \right) \\
& + \rho \frac{\mathrm{e}^{-v_n^2 - \frac{\omega^2}{4}}}{4\sqrt{\pi}} \left[\mathrm{e}^{v_n \omega} \left(1 - \frac{2v_n}{\omega} \right) + \mathrm{e}^{-v_n \omega} \left(1 + \frac{2v_n}{\omega} \right) \right].
\end{aligned}
\tag{22}
$$

A collision time is generated by solving the equation

$$\int_0^t \mathrm{d}t' \Phi(t') = -\ln(\xi_3). \tag{23}$$

Since the integral cannot be performed analytically, we use the Newton–Raphson method:

$$t_1 = t - \frac{\int_0^t \Phi(t') \, \mathrm{d}t' + \ln(\xi_3)}{\Phi(t)} \tag{24}$$

with an initial guess $t = -\frac{\ln(\xi_3)}{\Phi(0)}$. The procedure is iterative, i.e. t is substituted by t_1 in equation (24), etc until $\left| \int_0^{t_1} \Phi(t') \, \mathrm{d}t' + \ln(\xi_3) \right|$ is smaller than the required precision. In general the convergence is fast and only a few iterations are required. Occasionally, when Φ is small, the Newton–Raphson method oscillates between two 'stable' positions and there is no convergence. When this situation arises, we switch to a bisection procedure. With this modification, the method seems to be robust.

Once the time to collision has been selected, one updates the normal velocity of the centre of mass of the needle using equation (20).

In order to choose the position of the impact, one has to calculate the probability that the collision occurs at a distance x from the centre of mass of the needle, whatever the velocities of the bath particles, at a given time t

$$p(x|t) = \frac{\Phi(v_n + x\omega)}{\Phi(v_n, \omega)}, \qquad -1/2 \leqslant x \leqslant 1/2. \tag{25}$$

This probability is clearly not uniform over the length of the needle. But since it is concave, the maximum is obtained for $x = 1/2$ or $x = -1/2$ (if $v_n = 0$ the probability is a maximum at both ends). We select x using a standard acceptance–rejection method.

Once the position of the impact has been decided, one has to choose if the bath particle collides on the right- or left-hand side of the needle. The probability of the former event is

$$p(+|x, t) = \frac{\Phi_+(v_n + x\omega)}{\Phi(v_n + x\omega)}. \tag{26}$$

One chooses a random number between 0 and 1. If $\xi < p(+|x, t)$, the particle collides with a particle from the right, otherwise the collision is on the left.

Next the velocity of the colliding bath particle must be selected. The probability that the colliding particle has a velocity between v and $v + dv$ is $g_\pm(v, v_n + x\omega) \, dv$. It is even more important to sample this distribution carefully than in the one-dimensional case as more extreme velocities are encountered in this system.

Finally, the needle velocity and angular velocity are updated using

$$\mathbf{v_1'} = \mathbf{v_1} + \mathbf{n}\frac{\Delta p}{M} \tag{27}$$

$$I\omega' = I\omega + x\Delta p, \tag{28}$$

where

$$\Delta p = -\frac{(1 + \alpha)\mathbf{g} \cdot \mathbf{n}}{\frac{1}{m} + \frac{1}{M} + \frac{x^2}{I}}, \tag{29}$$

$\mathbf{n}$ is a unit vector normal to the length of the needle and $\mathbf{g} = \mathbf{v_1} - \mathbf{v} + \omega x\mathbf{n}$ is the relative velocity at the point of impact (the velocity of the colliding bath particle also changes, but we do not need to know the new value).

It is necessary to simulate a few hundred thousand to several million collisions in order to obtain good estimates for the properties of interest. The convergence of the simulation is slower when the mass of the needle is much bigger than the bath particle mass.

We have previously used this algorithm to confirm a kinetic theory prediction that, when the coefficient of restitution is smaller than unity, the temperature of the bath is larger than the translational granular temperature which is in turn larger than the rotational granular temperature [10].

Here we present new results for the cross-correlation between the two degrees of freedom of the needle as a function of the coefficient of restitution, α, and for different values of the mass ratio M/m. Specifically, we have calculated

$$R = \frac{\langle v^2\omega^2 \rangle}{\langle v^2 \rangle \langle \omega^2 \rangle}, \tag{30}$$

which is equal to 1 in equilibrium systems and obviously independent of the mass ratio. Conversely, one observes that for small mass ratios in an inelastic system, there is a positive correlation that increases with decreasing α: see figure 7. We expect this to be a generic feature of anisotropic granular particles in any dimension, regardless of the bath particle velocity distribution.

Unlike the one-dimensional model, where the velocity distribution of the intruder particle is Gaussian for all values of the coefficient of restitution, the translational and angular velocity distributions of the granular needle are never strictly Gaussian (except for elastic collisions). For a large range of values of M/m and α, however, the Gaussian is a very accurate approximation. It is only for a light needle and highly inelastic collisions that deviations start to become apparent: see figure 8.
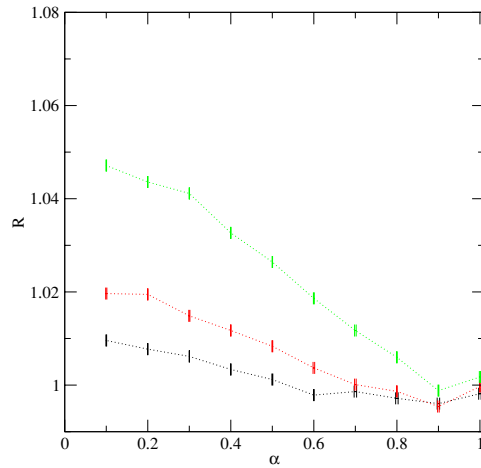
Figure 7. Correlation coefficient, equation (30), as a function of the coefficient of restitution for $M = 0.1, 0.5, 1$, top to bottom.
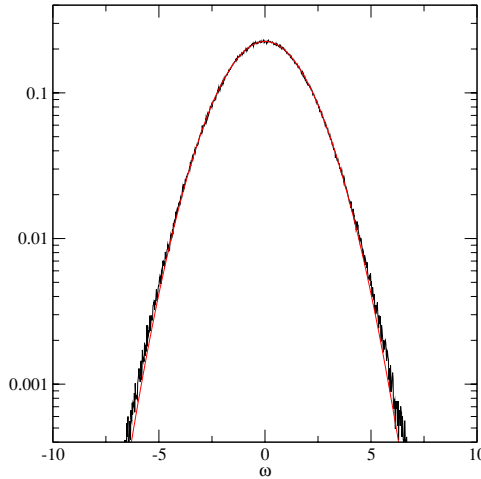

Figure 8. Angular velocity distribution for $M/m = 0.1$ and $\alpha = 0.1$. Noisy line: simulation with 5 000 000 collisions; smooth line: best-fit Gaussian.

4. DMSC versus Gillepsie algorithm

The two simulation methods provide an exact numerical solution of a Boltzmann equation (they can also be used for inelastic Maxwell models [15–17]). The DSMC algorithm has been described in several articles [4, 18]. For convenience we describe here the version that would be applied to the one-dimensional system discussed in section 3.1.

Velocities sampled from a Gaussian distribution, equation (14), are assigned to n_{bath} bath particles. A side of the intruder particle is then selected at random: $\sigma_{i1} = +1$ for a collision on the left, $\sigma_{i1} = -1$ for a collision on the right. A bath particle, i, is then selected randomly. The collision is accepted with probability $\Theta(v_{i1}\sigma_{i1})\omega_{i1}/\omega_{\text{max}}$, where $\Theta(x)$ is the Heaviside function, $\omega_{i1} = 2\rho|v_{i1}|$ and ω_{max} is an upper bound estimate of the probability that a particle

collides per unit time. If the collision is accepted a post-collisional velocity, computed from equation (17), is assigned to the intruder particle. If $\omega_{i1} > \omega_{max}$ the estimate of the latter is updated: $\omega_{max} \leftarrow \omega_{i1}$.

We have implemented this algorithm for the one-dimensional intruder described in section 3.1. We obtain the same results with comparable computational effort.

5. Conclusion

We have shown how the Gillespie algorithm can be used to obtain an exact numerical solution of the Boltzmann equation of an intruder particle in a bath of particles with an arbitrary velocity distribution. We used the method to obtain new results for a one-dimensional system consisting of an intruder particle in a bath with a power-law distribution. We also used it to demonstrate, for the first time, the presence of correlations between the translational and rotational momenta of an anisotropic particle.

Although the results presented here apply to the steady state, the method is equally valid for the transient case. It is clear that the Gillespie algorithm offers no significant computational advantage over the DSMC method for these intruder particle systems. It is of interest, however, that two apparently dissimilar methods can be applied to the same physical system. Finally, we note that, as with DSMC, the Gillespie method can be easily generalized to three-dimensional systems.

Acknowledgments

References

[1] Pöschel T and Luding S (ed) 2001 *Granular Gases* (Berlin: Springer)
[2] Pöschel T and Brilliantov N 2003 *Granular Gas Dynamics* (Berlin: Springer)
[3] Piasecki J, Talbot J and Viot P 2006 *Physica* A, at press
[4] Bird G 1994 *Molecular Gas Dynamics and the Direct Simulation of Gas Flows* (Oxford: Clarendon)
[5] Gillespie D T 1976 *J. Comput. Phys.* **22** 403–34
[6] Gillespie D T 1977 *J. Phys. Chem.* **81** 2340–61
[7] Dufty J W and Brey J J 2005 *New J. Phys.* **7** 20
[8] Brey J J, Ruiz-Montero M J and Moreno F 2005 *Phys. Rev. Lett.* **95** 098001
[9] Martin P A and Piasecki J 1999 *Europhys. Lett.* **46** 613
[10] Viot P and Talbot J 2004 *Phys. Rev.* E **69** 051106
[11] Gomart H, Talbot J and Viot P 2005 *Phys. Rev.* E **71** 051306
[12] Puglisi A, Visco P, Trizac E and van Wijland F 2006 *Phys. Rev.* E **73** 021301
[13] Feitosa K and Menon N 2002 *Phys. Rev. Lett.* **88** 198301
[14] Wildman R D and Parker D J 2002 *Phys. Rev. Lett.* **88** 064301
[15] Ben-Naim E, Machta B and Machta J 2005 *Phys. Rev.* E **72** 021302
[16] Ben-Naim E and Machta J 2005 *Phys. Rev. Lett.* **94** 138001
[17] Ben-Naim E and Krapivsky P 2003 *Granular Gas Dynamics* (Berlin: Springer) p 64
[18] Montanero J M and Santos A 2000 *Granular Matter* **2** 53